eJSSNT ALC '19 Conference

e-Journal of Surface Science and Nanotechnology **18**, 57−61 (2020)

Development of Simple Display-type VD-WAAEL Analyzer

Hiroki Momono,[a, †] Hiroyuki Matsuda,[b] László Tóth,[c] Hiroshi Daimon [d]

[a] *National Institute of Technology, Yonago College, 4448, Hikona, Yonago, Tottori 683-8502, Japan*
[b] *Institute for Molecular Science, 38 Nishigo-Naka, Myodaiji, Okazaki, Aichi 444-8585, Japan*
[c] *University of Debrecen, H-4032 Debrecen, Egyetem t'er 1., Hungary*
[d] *Toyota Physical and Chemical Research Institute, 41-1, Yokomichi, Nagakute, Aichi 480-1192, Japan*
[†] *Corresponding author: momono@yonago-k.ac.jp*

Received: 13 December, 2019, Accepted 18 February, 2020, Published 5 March, 2020

We have realized a simple and compact new two-dimensional electron analyzer "a VD-WAAEL analyzer" using a variable-deceleration-ratio wide-acceptance-angle electrostatic lens (VD-WAAEL). Using an electron gun and an angle measurement tool, we confirmed that a two-dimensional angular distribution could be measured at once over a large solid angle of ±45°. We also confirmed that energy analysis could be performed with an aperture. Here a high energy resolution of ~0.23% was obtained by using the aperture size of 0.8 mmϕ at the 40° position. Moreover, a magnified image of SUS316 #100 mesh was successfully measured. The magnification ratio was 25, which was in good agreement with the calculation.

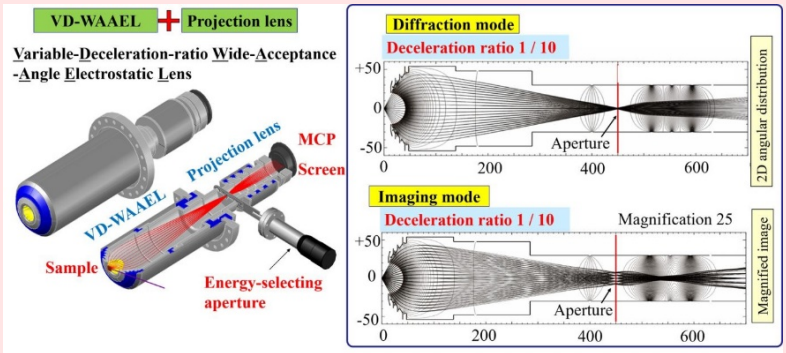

Keywords *VD-WAAEL; DELMA; Two-dimensional photoelectron spectroscopy*

I. INTRODUCTION

When a sample is irradiated by X-ray or UV (ultraviolet light) beam, photoelectrons from inner core states and valence bands are emitted. Then, fruitful information on surface electronic states and atomic structures can be obtained by measuring energy and angular distributions of emitted photoelectrons [1−3]. There are various approaches for this complete set [a two-dimensional (2D) (θ, φ) angular distribution and a kinetic energy E_k distribution at each angle] of the measurements. The angular-distribution measurement over an angle of 1π sr can be applied for band-structure analysis [4−6], photoelectron diffraction spectroscopy [7, 8], and photoelectron holography [9]. The ideal analyzer is the one having high energy resolution with a wide acceptance angle. Generally, a higher energy resolution in a deflection analyzer is achieved by reducing the kinetic energy of photoelectrons and introducing to a narrow slit at the entrance of the analyzer. However, there is a trade-off relationship between a high energy resolution and a high signal intensity because a highly decelerated electrons cannot be focused to a small area with a small divergence angle. In addition, when the acceptance angle increases, it is difficult to focus the electrons to a small area by conventional electron lenses because the spherical aberration of the electron lens becomes very high.

The most common concentric hemispherical analyzer (CHA) has high-energy-resolution capabilities, but it is not efficient for the angular distribution measurements because its acceptance angle is limited to ±15° × ±0.5° typically.

For efficient angular distribution measurements, several wide-angle 2D electron analyzers have been developed, e.g., a display-type elliptical mirror analyzer [10], a display-type spherical mirror analyzer (DIANA) [11, 12], a display-type ellipsoidal mesh analyzer (DELMA) [13−17], and retarding-field analyzer (RFA) [18]. Among them, DIANA can measure the photoelectron angular distribution efficiently with a wide ±60° × ±60° acceptance angle with no distortion.

However, the energy resolution of the DIANA is about 1%, which is not enough to measure chemical-shift-resolved photoelectron diffraction patterns. The next mentioned display-type analyzer is the DELMA that has a microscopy function with a high energy resolution in addition to the feature of the DIANA. The DELMA consists of a wide-acceptance-angle electrostatic lens (WAAEL), a transfer lens system, and a CHA (VG Scienta R4000). The WAAEL can accept the electrons with wide angles of ±50° × ±50° with reducing spherical aberrations to almost zero [19–23]. The DELMA system can measure high-energy-resolution wide range 2D angular distributions by a deflector-scanning method. Here, the ±50° × ±50° 2D angular distribution formed at the detector plane of the DELMA, which is the input plane of the CHA, is scanned using electrostatic deflectors, and many 1D (±12.5° × ±0.5°) patterns obtained by the CHA are combined to construct the 2D pattern. These slices, then, can be combined to reconstruct the 2D real- or *k*-space images of the sample. Although the DELMA solved DIANA's low-energy-resolution problem, it has not been used widely due to its complicated structure, a large size, and a relatively high cost. Another approach of the 2D analyzer is to use a PEEM technique [24], where a high accelerating voltage around 20 kV is applied between the sample and an objective lens. A very wide acceptance angle of almost ±90° (2π sr) is achieved for photoelectrons in UV and extreme UV energy ranges. However, the acceptance angle rapidly decreases with increasing the kinetic energy, and the angular range is not enough to study photoelectron diffraction or holography.

In this paper, we report on the realization of a new wide-angle 2D electron analyzer proposed in Ref. 25. This analyzer is based on the technique of the DELMA but is fundamentally different in the objective lens design. In the DELMA, a WAAEL of an einzel type was used as objective lens. This means that the electrons leave the lens with the same kinetic energies as those at its entrance. As a result, for the electrons with a kinetic energy of E_k = 1 keV, high voltages up to around 5 keV are applied to the lens system after the objective lens to focus the electrons. The applied voltages linearly increase with the electron kinetic energy. This limits the kinetic energy range in which the DELMA can be used. We also mention that the DELMA had a somewhat complicated lens system after the objective lens. The present development uses a variable-deceleration-ratio WAAEL (VD-WAAEL) (Figure 1) which is an improvement of the deceleration-type WAAEL in Ref. 20. The VD-WAAEL allows us to simplify the lens system following the objective lens.

The left side of the abstract figure shows a simplest 2D electron analyzer (a VD-WAAEL analyzer) that is just a combination of the objective lens, projection lens, and a screen, along with an energy-selecting aperture. The VD-WAAEL analyzer has both diffraction and imaging modes (right-top and right-bottom images in the abstract figure, respectively). It can switch these modes just by changing voltages of lenses as with the DELMA, as shown in the abstract figure. In the imaging mode figure, electrons emitted from a 1-mm sample area are considered, with trajectories starting from z = 0 and x = −0.5, −0.25, 0.0, +0.25, +0.5 mm (z is a horizontal axis and x is a vertical axis). The imaging mode is used to display a magnified image of the sample on a screen, and it is useful to see the sample surface. Moreover, in the VD-WAAEL system, the deceleration ratio can be changed in a wide range without changing the electron focusing at the exit of the lens. This

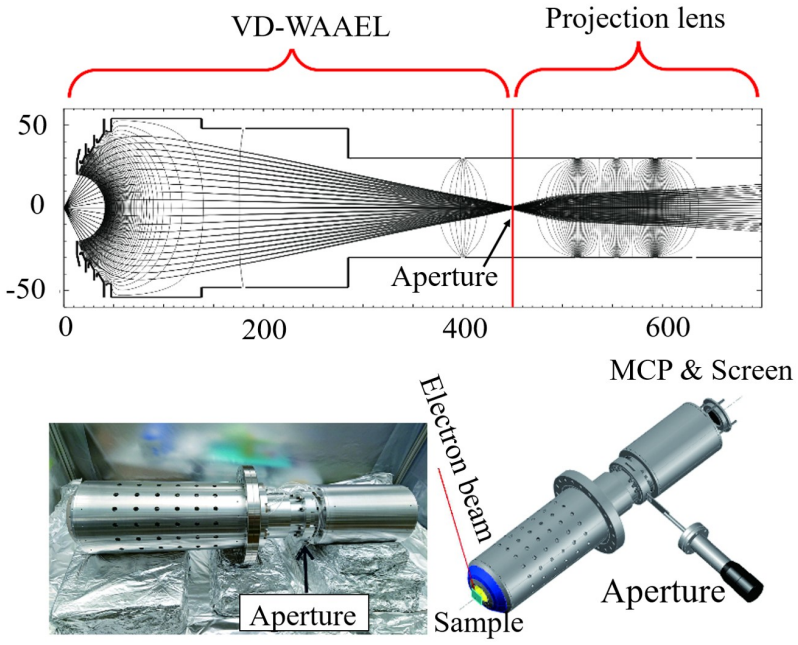

Figure 1: Wide-angle display-type 2D VD-WAAEL analyzer.

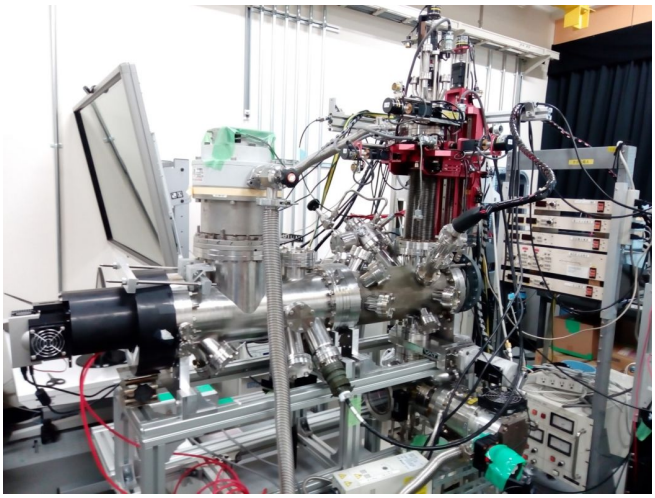

Figure 2: Whole system of the 2D VD-WAAEL analyzer.

feature should be useful for applying the 2D electron analyzer in a wide range of electron kinetic energies. A high deceleration ratio is necessary for hard X-ray photoelectron spectroscopy.

II. INSTRUMENTATION

Figure 1 shows the drawings and photographs of the wide-angle display-type 2D VD-WAAEL analyzer that we have developed. The objective lens is a VD-WAAEL, and a projection lens is combined with it. The exit slit of the VD-WAAEL is a round hole with a diameter of 15 mm, the center of which is on the optical axis. An aperture plate is inserted along a guide groove to set an aperture at the center of the exit hole. The plate has five circular apertures with diameters of 5, 3, 1.8, 1.1, and 0.8 mm. A micro-channel plate (MCP) & screen is mounted after the final electrode of the projection lens. The VD-WAAEL is mounted on an ICF 203 (conflat) flange with the projection lens. The distance between the sample and the MCP is 700 mm in the present design, which is shown in Ref. 25. The working distance (the distance between the sample and the objective lens entrance) is 9.5 mm. The electron trajectories shown are those calculated in the diffraction mode in the case where the deceleration ratio ε is 1/10. Here, we define ε by $\varepsilon = E_f/E_i$, where E_i and E_f are the electron kinetic energies at the entrance and the exit of the VD-WAAEL, respectively. The size of the diffraction pattern obtained at the screen is expected to be around 30 mm in the case ε = 1/10. The measurement mode can be changed to the imaging mode by changing the voltages applied to the projection lens, where a magnified sample image can be obtained. The magnification is around 25 in the case ε = 1/10. Figure 2 shows a whole system of the constructed 2D VD-WAAEL analyzer. The VD-WAAEL analyzer shown in Figure 1 was put into a cylindrical chamber with ICF203 flanges with a length of 1000 mm. The chamber contains the VD-WAAEL, the projection lens, and the MCP & screen. The cylinder part of the chamber is covered by a μ-metal shield with a thickness of 1 mm. Another μ-metal shield with a thickness of 1 mm is put into the chamber to cover the VD-WAAEL and the projection lens. The VD-WAAEL is thus surrounded by double μ-metal shields inside and outside the chamber. A five-axis manipulator is put on an ICF152 port in the vertical direction, and a load-lock chamber is put on an ICF114 port on the opposite side. Dry vacuum pumps and TMPs (turbo molecular pump) are installed at the load-lock chamber and the main chamber. An electron gun is installed on an ICF70 port, directed to the sample with an angle of 15° from the sample plane. An X-ray source will be installed later.

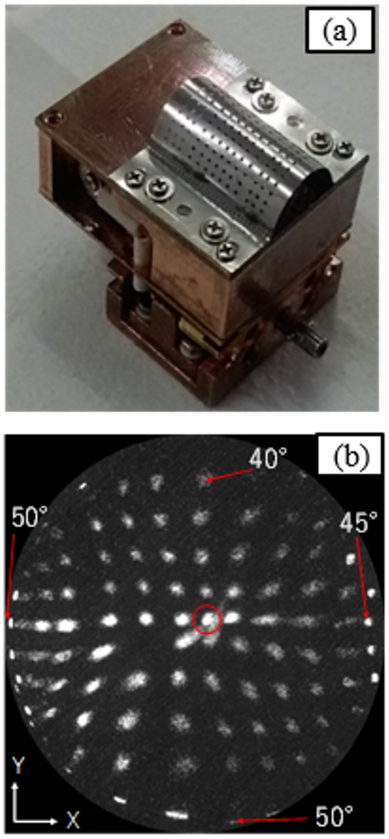

Figure 3: (a) Special tool to measure angular distribution. (b) Angular distribution measured using an electron gun.

III. RESULTS AND DISCUSSION

Figure 3(a) is a special tool to measure angular distribution of the VD-WAAEL analyzer. There are arrays of holes on the barrel-shaped plane. First, the pass energy of VD-WAAEL was adjusted to 1 keV which is the same as the energy of the electron beam emitted from the electron gun. Figure 3(b) shows the result of angle measurement using the electron gun and the angle measurement tool when ε = 1/10 and the aperture size was 0.8mmϕ. The central red circle represents the direction of the lens axis. The vertical direction of the image is defined as a Y axis and the horizontal direction is defined as an X axis as shown in Figure 3(b).

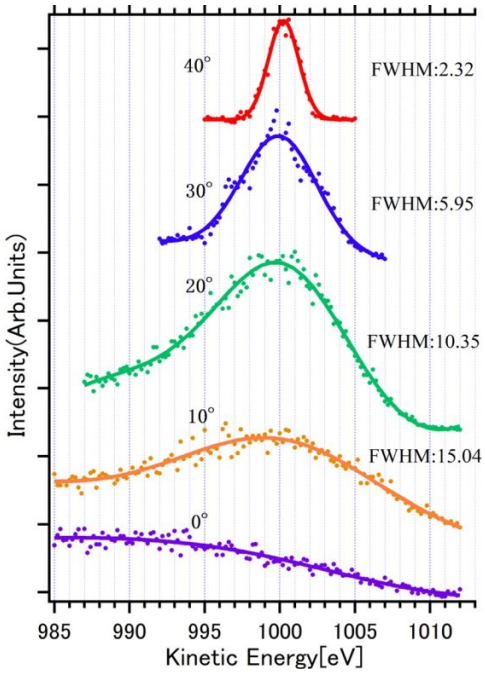

Figure 4: Energy spectra taken from θ = 40° to 10° along the Y axis.

The distance between the bright spots along the X and Y axes corresponds to 10°. Hence, the acceptance angle observed by the VD-WAAEL analyzer in the X and Y axes was confirmed to be ±45°.

The energy resolution was estimated by taking energy spectra (a pass-energy dependence of the spot intensity) for θ from 40° to 10° along the Y axis, where θ is the angle from the central axis, since the electron beam spreads in the X direction. The obtained spectrum is shown in Figure 4. The energy resolution ($\Delta E/E$) was estimated for each peak in Figure 4 by estimating full width at half maxima (FWHMs) of these peaks and was plotted in Figure 5 with respect to θ. $\Delta E/E$ decreases with increasing θ, and the best energy resolution of the VD-WAAEL analyzer was estimated to be 0.23% at θ = 40°. In the case of the focus-defocus-type energy analyzer such as the WAAEL or the VD-WAAEL, the energy resolution is reasonably good in a wide angular range except close to the central axis. At the optical axis (at 0°), this type of the focus-defocus analyzer cannot resolve photoelectron energy since photoelectrons of all energies can pass through. The energy resolution of the VD-WAAEL analyzer strongly depends on the aperture size, and the size or shape of electron beam on the sample surface as described in Ref. 25. Even though the size of the electron beam in this experiment is ten times larger than that used in the simulation in Ref. 25, the obtained energy resolution here is not so different from the estimated value in Ref. 25. The angular resolution was estimated to be about 2.5° from the line profile of the peak in Figure 4. The horizontal angular resolution is worse than the vertical resolution because the electron beam was incident from the left to right in the figure and the beam spot on the sample was elongated in horizontal direction. It is considered that the reason why the angular resolution in the measurement was poor is that the spot size of the electron beam was larger than 1 mm. In order to improve the angular resolution, it is necessary to narrow the spot size of the electron beam and to use a smaller aperture diameter.

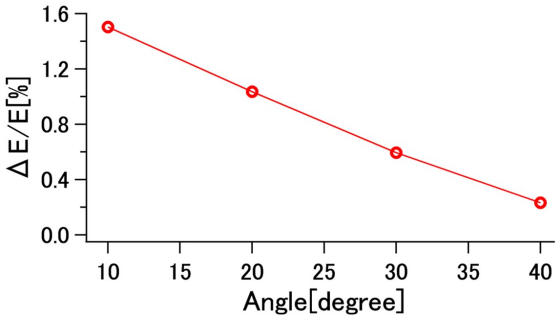

Figure 5: Relative energy resolution with respect to θ.

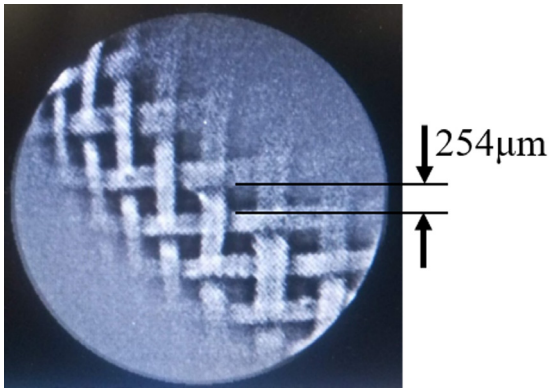

Figure 6: Magnified image with ε = 1/20 and aperture size of 0.8mmϕ.

The imaging capability of the VD-WAAEL analyzer was confirmed by measuring a magnified image from a mesh sample (SUS316 #100) when ε = 1/20 and 0.8 mmϕ aperture. The obtained image is shown in Figure 6. A high deceleration ratio is necessary in the imaging mode to suppress the voltage applied to the projection lens, therefore we selected ε = 1/20. This image was formed by elastically scattered electrons with a kinetic energy of 1 keV. The mesh pattern was observed clearly, and the magnification ratio was between 12 and 33 times, which is in good agreement with the calculated magnification ratio of 25 in Ref. 25. The origin of the difference of the magnification ratio is considered to be the tilted mesh sample orientation. The surface-normal direction from the optical axis of the VD-WAAEL was tilted by several degrees for the mesh surface to be shined by the electron beam properly. The lateral resolution was about 40 μm estimated by the cut-off of the wire image.

IV. CONCLUSIONS

We have realized a simple and compact new display-type electron energy analyzer using a VD-WAAEL (variable-de-

celeration-ratio wide-acceptance-angle electrostatic lens). Using an electron gun and an angle measurement tool, we confirmed that a two-dimensional angular distribution can be measured at once over a large solid angle of ±45° × ±45°. We also confirmed that the energy analysis can be performed with an aperture. Here, a high energy resolution of ~0.23% was obtained by using the aperture size of 0.8 mmϕ at the θ = 40° position. Finally, a magnified image of SUS316 #100 mesh was successfully measured with a magnification ratio of around 25 times. These performances are in good agreement with calculated values in Ref. 25. Hence, it can be concluded that we could succeed to develop a new simple display-type VD-WAAEL analyzer.

Note

This paper was presented at the 12th International Symposium on Atomic Level Characterizations for New Materials and Devices '19 (ALC '19), in conjunction with the 22nd International Conference on Secondary Ion Mass Spectrometry (SIMS-22), Miyako Messe, Kyoto, Japan, 20–25 October, 2019.

References

[1] S. Hüfner, *Photoelectron Spectroscopy* (Springer-Verlag, Berlin, Heidelberg, 2003) Chap. 4.
[2] F. Matsui, T. Matsushita, F. Z. Guo, and H. Daimon, Surf. Rev. Lett. **14**, 637 (2007).
[3] H. Daimon, J. Phys. Soc. Jpn. **87**, 061001 (2018).
[4] F. Matsui, Y. Hori, H. Miyata, N. Suganuma, H. Daimon, H. Totsuka, K. Ogawa, T. Furukubo, and H. Namba, Appl. Phys. Lett. **81**, 2556 (2002).
[5] H. Daimon and F. Matsui, Prog. Surf. Sci. **81**, 367 (2006).
[6] N. Takahashi, F. Matsui, H. Matsuda, Y. Hamada, K. Nakanishi, H. Namba, and H. Daimon, J. Electron Spectros. Relat. Phenomena **163**, 45 (2008).
[7] S. Fukami, M. Taguchi, Y. Adachi, I. Sakaguchi, K. Watanabe, T. Kinoshita, T. Muro, T. Matsushita, F. Matsui, H. Daimon, and T. T. Suzuki, Phys. Rev. Appl. **7**, 064029 (2017).
[8] Y. Kato, D. Tsujikawa, Y. Hashimoto, T. Yoshida, S. Fukami, H. Matsuda, M. Taguchi, T. Matsushita, and H. Daimon, Appl. Phys. Express **11**, 061302 (2018).
[9] T. Matsushita, F. Matsui, H. Daimon, and K. Hayashi, J. Electron Spectros. Relat. Phenomena **178–179**, 195 (2010).
[10] D. E. Eastman, J. J. Donelon, N. C. Hien, and F. J. Himpsel, Nucl. Instrum. Methods **172**, 327 (1980).
[11] H. Daimon, Rev. Sci. Instrum. **59**, 545 (1988).
[12] H. Daimon, Phys. Rev. Lett. **86**, 2034 (2001).
[13] K. Goto, H. Matsuda, M. Hashimoto, H. Nojiri, C. Sakai, F. Matsui, H. Daimon, L. Tóth, and T. Matsushita, e-J. Surf. Sci. Nanotechnol. **9**, 311 (2011).
[14] E. Ikenaga, M. Kobata, H. Matsuda, T. Sugiyama, H. Daimon, and K. Kobayashi, J. Electron Spectros. Relat. Phenomena **190**, 180 (2013).
[15] H. Matsuda, K. Goto, L. Tóth, M. Morita, S. Kitagawa, F. Matsui, M. Hashimoto, C. Sakai, T. Matsushita, and H. Daimon, J. Electron Spectros. Relat. Phenomena **195**, 382 (2014).
[16] Y. Hashimoto, M. Taguchi, S. Fukami, H. Momono, T. Matsushita, H. Matsuda, F. Matsui, and H. Daimon, Surf. Interface Anal. **51**, 115 (2019).
[17] M. Taguchi, F. Matsui, N. Maejima, H. Matsui, and H. Daimon, Surf. Sci. **683**, 53 (2019).
[18] T. Muro, T. Ohkochi, Y. Kato, Y. Izumi, S. Fukami, H. Fujiwara, and T. Matsushita, Rev. Sci. Instrum. **88**, 123106 (2017).
[19] H. Matsuda, H. Daimon, M. Kato, and M. Kudo, Phys. Rev. E **71**, 066503 (2005).
[20] H. Matsuda and H. Daimon, Phys. Rev. E **74**, 036501 (2006).
[21] H. Matsuda, H. Daimon, L. Tóth, and F. Matsui, Phys. Rev. E **75**, 046402 (2007).
[22] L. Tóth, H. Matsuda, T. Shimizu, F. Matsui, and H. Daimon, J. Vac. Soc. Jpn. **51**, 135 (2008).
[23] L. Tóth, H. Matsuda, F. Matsui, K. Goto, and H. Daimon, Nucl. Instrum. Methods Phys. Res. A **661**, 98 (2012).
[24] E. Bauer, J. Electron Spectros. Relat. Phenomena **185**, 314 (2012).
[25] H. Matsuda, L. Tóth, and H. Daimon, Rev. Sci. Instrum. 89, 123105 (2018).

Published by The Japan Society of Vacuum and Surface Science